Scripta Materialia 223 (2023) 115062

Contents lists available at ScienceDirect

Scripta Materialia

journal homepage: www.journals.elsevier.com/scripta-materialia

Viscoelasticity-induced structure anisotropy in amorphous materials

Ruixin Sheng [a], Zhinan An [b,1], Andew C.-P. Chuang [c], Xie Xie [b], Peter K. Liaw [b,*], Yang Tong [a,*]

[a] Institute for Advance Studies in Precision Materials, Yantai University, Yantai 264005, China
[b] Department of Materials Science and Engineering, The University of Tennessee, Knoxville, TN 37996, USA
[c] Argonne National Laboratory, Lemont, IL 60439, USA

ARTICLE INFO

Keywords:
Metallic glass
Amorphous selenium
Structural anisotropy
Synchrotron X-ray diffraction

ABSTRACT

Viscoelasticity-induced structural change in $Zr_{55}Cu_{30}Ni_5Al_{10}$ metallic glass (Zr-MG) and amorphous selenium (a-Se) is investigated using synchrotron X-ray diffraction. By analyzing the two-dimensional diffraction pattern, two types of structural anisotropy with the feature of the residual elastic strain or heterogeneous intensity of diffraction rings are revealed. The origin of the structural anisotropy is attributed to the topological rearrangement in the Zr-MG and conformation rearrangement in the a-Se. Our findings bring a structural identity to the phenomenological structureless deformation defect widely used in different amorphous materials.

Mechanical response of materials is critically determined by their crystal structure. Making a direct link between the structure and mechanical behaviors in amorphous materials, however, is challenging since deformation defects are not well defined in such materials [1]. Viscoelasticity, a local stress-relaxation behavior, is often linked to so-called "flow defects" in metallic glasses (MGs) based on the observation of viscoelastic-to-viscoplastic transition [2–4]. Furthermore, the transition of inhomogeneous-to-homogeneous deformation in MGs is determined by the relaxation time of viscoelasticity [2,5]. Therefore, the characterization of the local structural change induced by viscoelasticity is the key to understanding deformation defects and hence the deformation mechanisms of amorphous materials.

Viscoelasticity in a variety of amorphous materials can be well described by a complex combination of mechanical analogs, the Hookean elastic spring and Newtonian damper, but its corresponding structural information is rarely studied because "flow defects" and their motion in amorphous materials is hardly captured, unlike dislocations in crystalline materials. Instead, a phenomenological model [6,7] proposed that flow defect regions, shear transformation zones, are linked to unstable atomic sites with extra volume (named free volume) and their surrounding atoms, which can be activated under shear. The free-volume model quantitatively reproduces the experimental stress-strain curves for polymers and amorphous alloys [8,9]. Indeed, the amorphous materials' density slightly decreases upon annealing in support of the free-volume concept [10–12]. Such phenomenological model has been widely adopted across all amorphous materials, but the viscoelastic response at the microscopic level for different amorphous materials is more complex due to the difference in both the length scale and rearrangement mode of their structural units.

The structural unit of amorphous materials is diverse in geometry and length scale. Silica glass has a tetragonal structural unit forming a network of rings of different sizes [13,14], amorphous polymers consist of polymer chains with varying lengths, and MGs have structural units of densely packed atomic clusters [15,16]. Besides dramatically different structural units, the packing density of their structural units changes from one amorphous material to another, and the packing density even in the same material is heterogeneous, considering the geometrical frustration with a periodic structure [16]. Moreover, Cohen and Turnbull [17] pointed out that the free-volume size in liquid metals was around 10% of the average atomic size while 70% of the average atomic volume in van der Waals liquid. All above-mentioned differences, however, are smeared by the free-volume model. Furthermore, an integration method of the local structure characterization and molecular dynamics (MD) simulations revealed that both the free volume (sites under a negative atomic pressure) and anti-free volume (sites under a positive atomic pressure) are created through a topological-rearrangement process of cutting and forming bonds when MGs are homogeneously deformed around the glass-transition temperature (T_g) [4,5]. This topological rearrangement is the elementary excitation event [18] in the "flow defects" associated with viscoelastic responses in MGs. Still, it is unknown whether viscoelasticity in nonmetallic amorphous systems involves a similar process of the

* Corresponding authors.
E-mail addresses: pliaw@utk.edu (P.K. Liaw), yt1@ytu.edu.cn (Y. Tong).
[1] Deceased.

https://doi.org/10.1016/j.scriptamat.2022.115062
Received 21 June 2022; Received in revised form 11 September 2022; Accepted 17 September 2022
Available online 28 September 2022

topological rearrangement and defect creation.

To study the viscoelasticity-induced structural change, two prototypical amorphous materials, $Zr_{55}Cu_{30}Ni_5Al_{10}$ metallic glass (Zr-MG) and amorphous selenium (a-Se), were chosen in the present work. A monatomic a-Se, similar to a narrow molecular weight distribution of polymer, has a well-defined covalent-bound chain structure. The metallic-bound Zr-MG has a densely packed structure. Viscoelasticity was introduced into both samples through the thermal-mechanical creep. Zr-MG (T_g = 434 °C) was crept under uniaxial compressive stress of 800 MPa at 380 °C for 1 h, and a-Se (T_g = 30 °C) was crept under a compressive stress of 30 MPa at 35 °C for 5 min. After creep, samples were cooled down to room temperature under stress. Then structural study was performed on both the as-cast (denoted as a non-deformed state) and crept (denoted as a deformed state) samples using synchrotron X-ray with the beam energy of 100 keV (λ = 0.12398 Å) at the beamline ID-1, Argonne National Laboratory. A two-dimensional (2-D) detector having 2048 * 2048 pixels with a 200 * 200 μm^2 pixel size was used to collect diffraction patterns. The detector was placed ~35 cm behind the sample stage. Calibration was performed, using the CeO_2 powder standard. The FIT2D software [19] was used to correct for the beam polarization and the dark current.

To see the structural change induced by viscoelasticity, the difference of 2-D diffraction patterns between the deformed and non-deformed state is plotted in Fig. 1. Compared with the as-cast state, diffraction rings of the crept Zr-MG are no longer isotropic since diffraction rings are elongated along the Y axis, the loading direction, and compressed in the X direction as shown in Fig. 1a. A similar phenomenon was also observed in other MGs after creep or high-temperature deformation [4,20]. Distortion of diffraction rings observed in the free-standing Zr-MG indicates that some residual elastic strain was frozen into the sample after creep. In Fig. 1b, the diffraction rings of the crept a-Se are seemingly distorted, too. To further quantitatively analyze the difference in the 2-D diffraction pattern, elastic strain was determined with respect to the shift of diffraction peaks [21,22], $\varepsilon_{nth}(\varphi) = (Q^0_{nth}(\varphi) - Q_{nth}(\varphi))/Q^0_{nth}(\varphi)$, where $Q = 4\pi\lambda sin\theta$ is a diffraction vector, *nth* indexes the diffraction rings, φ indicates the angular dependence, and the superscript, 0, refers to the as-cast reference state. With an accuracy of $\Delta\varepsilon = \pm$ 0.1%, we obtained $\varepsilon_{1st}(90^\circ) = -$ 0.3% for the crept Zr-MG but $\varepsilon_{1st}(90^\circ) = 0\%$ for the crept a-Se. This zero elastic strain reveals that the first peak of the crept a-Se does not shift at all. Then, one question is raised: what causes the difference in Fig. 1b?

Then, we examined the one-dimensional diffraction profile, $I(Q)$, of the as-cast and crept samples by integration their 2-D diffraction patterns. Fig. 2 presents the diffraction profile of as-cast samples and the diffraction profile difference between crept and as-cast samples along two φ angles, $\Delta I(Q,\varphi)$. From Fig. 2a, we can see that the positions of intensity maxima and minima in $\Delta I(Q,0^\circ)$ and $\Delta I(Q,90^\circ)$ are not overlapped with the $I(Q)$ of the non-deformed Zr-MG sample. For the crept a-Se, the maxima and minima of $\Delta I(Q,0^\circ)$ and $\Delta I(Q,90^\circ)$ are well aligned with the peaks of $I(Q)$ (Fig. 2b), indicating that the positions of diffraction peaks have negligible change after creep. The feature in Fig. 1b essentially is caused by the intensity anisotropy of each diffraction rings in $I(Q)$, similar to the diffraction pattern of alloys with textures [23]. The Texture in alloys is the preferred distribution of the crystallographic orientation of grains [24]. To our knowledge, this anisotropic intensity diffraction pattern in the crept a-Se currently is firstly observed.

Both amorphous materials were crept homogeneously without any shear localization (e.g., shear bands observed in a metallic glass after heterogeneous deformation at room temperature [25]). The elastic strain should be recovered immediately when an external stress was removed. Therefore, the structural anisotropy in both crept Zr-MG and a-Se must be induced by time-dependent viscoelasticity because of the kinetical arrest of the recovery of the viscoelastic strain during the cooling process [20,26,27]. Apparently, the residual elastic strain in the deformed Zr-MG should be stabilized by the local structural change associated with viscoelasticity whereas the observed anisotropic intensity in the crept a-Se must be attributed to different types of structural changes induced by viscoelasticity.

To further understand the anisotropy in local structural change induced by viscoelasticity, we conducted a spherical harmonic expansion separate the isotropic part of the structure function, $S^0_0(Q)$, and the anisotropic part, $S^0_2(Q)$, from the total structure function, $S(\boldsymbol{Q})$,

$$S(\boldsymbol{Q}) = \sum_{l,m} S^m_l(Q) Y^m_l\left(\frac{\boldsymbol{Q}}{Q}\right).$$

Here, Y^m_l is spherical harmonics, $\boldsymbol{Q} = 4\pi sin\theta/\lambda$ the diffraction vector, and θ diffraction angle. Then, they are converted to the isotropic pair distribution function (PDF), $g^0_0(r)$, and the anisotropic PDF, $g^0_2(r)$, through the spherical Bessel transformation, to study the structural change induced by shear stress:

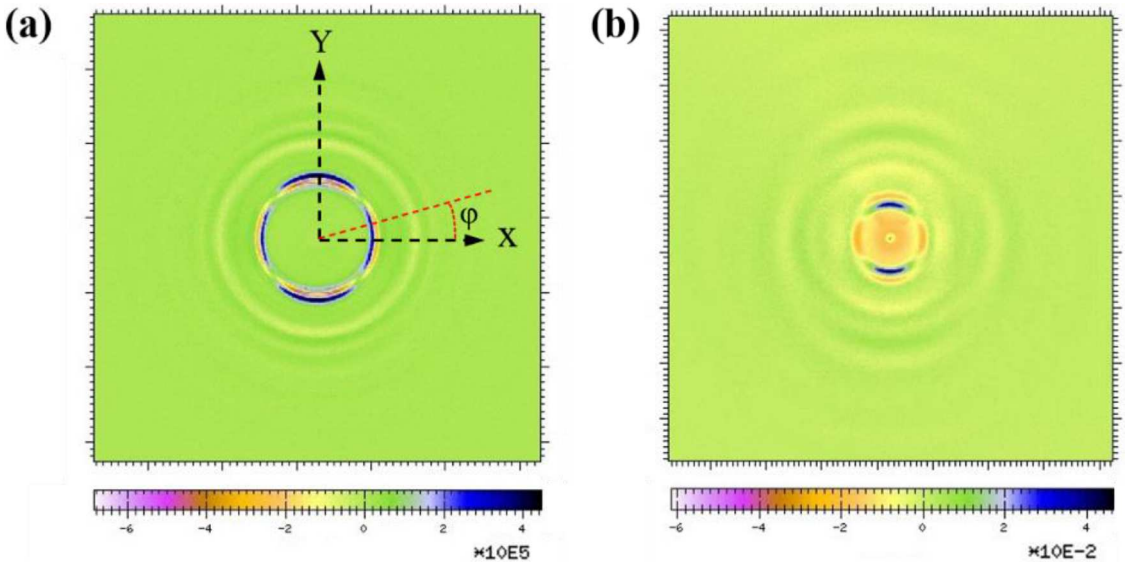

Fig. 1. Difference of 2-D diffraction pattern between the crept and non-deformed Zr-MG(a) and a-Se(b). The X and Y axes are perpendicular and parallel to the loading direction, respectively.

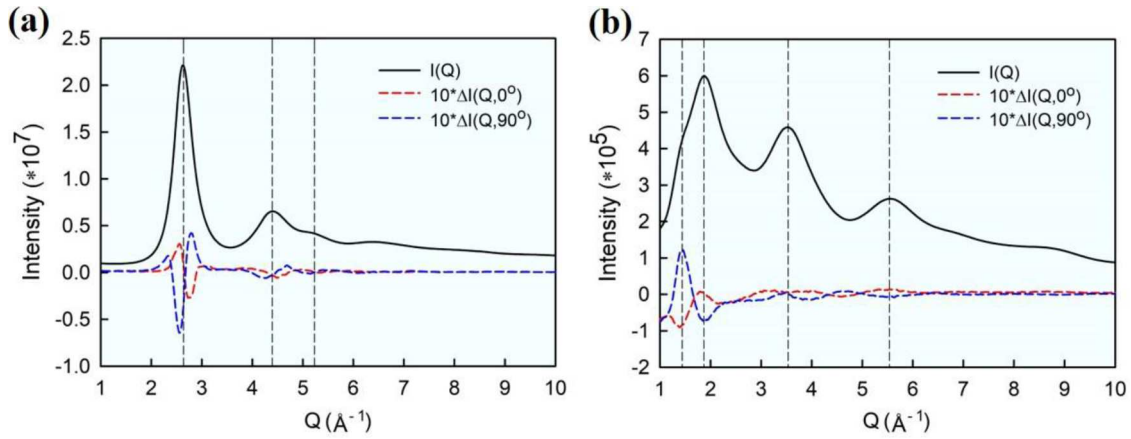

Fig. 2. Integration of 2-D diffraction pattern for the crept Zr-MG(a) and a-Se(b). The difference of $I(Q,\varphi)$ between crept and non-deformed states, $\Delta I(Q,\varphi)$, along $\varphi = 0^\circ$ and 90° is shown in the bottom. The vertical dash-line highlights the position of the diffraction peaks and subpeak. Please add a light background color to beautify each figure.

$$g_l^m(r) = \frac{i^l}{2\pi^2\rho_0}\int S_l^m(Q)J_l(Qr)Q^2dQ,$$

where ρ_0 is the atomic density of MGs, and $J_l(x)$ the spherical Bessel function. More details about this procedure can be found in refs [26–28]). Note that the isotropic PDF, $g_0^0(r)$, reflecting a volume change, and anisotropic PDF, $g_2^0(r)$, containing the information about the shear-induced structural change, from the total PDF. We firstly examined the volume change of the crept Zr-MG and a-Se samples by comparing the $g_0^0(r)$ of the crept sample with the as-cast sample, and their difference, $\Delta g_0^0(r)$, is shown in the upper panel of Fig. 3a and b together with error from the statistics and instrument. $\Delta g_0^0(r)$ in Fig. 3a indicates that the peaks of the $g_0^0(r)$ do not shift, but the peak height decreases. This characteristic changes in $g_0^0(r)$ are typical evidences of structural rejuvenation in MGs observed many times before [4,29], consistent with the free volume (atomic sites under expansion) and anti-free volume concepts (atomic sites under compression) [30]. For the a-Se case, $\Delta g_0^0(r)$, is comparable with the measurement uncertainty, indicating no volume change in the crept a-Se. Materials' volume changes when a hydrostatic stress is applied to stretch or compress an atomic bond, which causes a typical peak shift in $g_0^0(r)$ [14,28,31], but our crept samples do not involve net volume change but fluctuation of local density.

Our former study has shown that $g_2^0(r)$ is a powerful tool to characterize both the size and density of deformation defects in MGs [5]. For a solid under uniform elastic deformation, i.e., affine deformation, $g_2^0(r)$ is

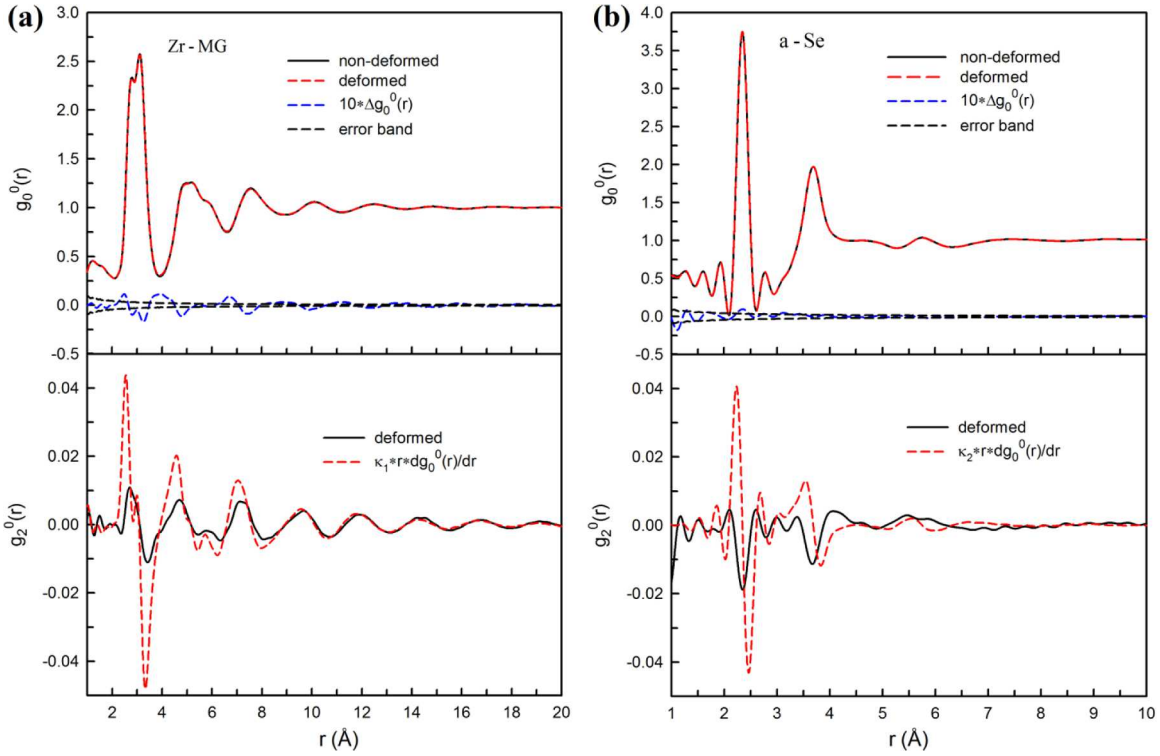

Fig. 3. The isotropic component,$g_0^0(r)$, and anisotropic component, $g_2^0(r)$, for the crept Zr-MG(a) and a-Se(b). In the upper panel, a comparison of $g_0^0(r)$ between the crept and as-cast state is also shown, and their difference amplified ten times is plot against the error from the statistics and instrument. In the lower panel, the $g_2^0(r)$ of the crept sample is compared with the ideal case of the affine deformation calculated from Eq. (1).

proportional to the first derivative of $g_0^0(r)$ as

$$g_2^0(r) = \varepsilon_{ela}\frac{1}{\sqrt{5}}\frac{2(1+\nu)}{3}r\frac{dg_0^0(r)}{dr} \quad (1)$$

where ε_{ela} is the elastic strain, and ν is the Poisson's ratio [26,28]. If deformation defects in MGs are activated, the local elastic strain is relaxed because of local topological rearrangements. Thus, the observed $g_2^0(r)$ cannot be fitted by a single elastic strain using Eq. (1). The lower panel in Fig. 3a presents the fitting in high r range representing the elastic behavior in matrix, but the low r range cannot be fitted simultaneously. However, the peak shape of the fitting (red dash line in the lower panel of Fig. 3a) and measured curves remain the same, and smaller elastic strain must be used to fit the measured curve, indicating the relaxed elastic strain in localized flow defects. Details about this fitting can be found in refs [5,28]. The intensity deviation below a characteristic value of ~ 9 Å in the observed $g_2^0(r)$ illustrates that the elastic strain is relaxed underneath the third atomic shell, which is the average radius of a viscoelastic event or flow defect. The uniform long-range elastic strain above 9 Å demonstrates that flow defects are confined within an elastic matrix, which can generate a back stress to force them to return to their initial configuration.

Polymer-like a-Se is viscoelastic to a great extent around the glass-transition temperature, but the lower panel of Fig. 3b shows that the observed $g_2^0(r)$ has a distinct shape and phase from the first derivative of $g_0^0(r)$ over the range presenting the clear structural information. Instead, the intensity minima of the measured $g_2^0(r)$ match the peaks of $g_0^0(r)$ in positions indicating that the bond length of intra-chains does not change, and the average distance between inter-chains is also maintained. The first peak of the $g_0^0(r)$ of the crept a-Se represents the distribution of intra-chain bond distances [32]. A large intensity change in the $g_2^0(r)$ corresponding to the first peak of the $g_0^0(r)$ indicates that the intra-chain nearest neighboring atoms make a major contribution to the viscoelasticity. Additionally, the second peak (at 3.68 Å) of $g_0^0(r)$ in the upper panel of Fig. 3b consists of two peaks associated with inter-chain and intra-chain atomic distributions, respectively [32]. The nearest inter-chain atomic distance locates at the left side of the second peak, and the second intra-chain nearest atomic distance locates exactly at the maximum of the second peak [32]. Again, the intensity change of the second peak of the $g_2^0(r)$ confirmed that viscoelasticity in a-Se mainly involves the change of the intra-chain Se atoms. Different from the MGs, viscoelasticity in the a-Se has no assistance from the residual elastic stress to recover its initial state.

Experimental and MD simulation results [33,34] proved that viscoelasticity in MGs is associated with bond-orientation anisotropy caused by the topological rearrangement in the form of bond cutting and formation. Such a bond switch is an elementary event in amorphous alloys [18]. For affine deformation, atomic bonds shrink along the compressive loading axis and extend in the perpendicular direction, forming a uniform elastic field. However, the local topological rearrangement relaxes this uniform elastic field by forming more bonds in the compressive direction while cutting some bonds in the perpendicular direction [33], as schematically exhibited in Fig. 4a. When such topologically-rearranged regions are stored in samples after fast cooling, a back stress is generated to balance the elastic stress in the elastic matrix. The memory effect from the confinement of the elastic matrix is lost if percolation occurs among such topological defects, leading to a viscoplastic-flow behavior [3,4,7].

Viscoelasticty in polymers is often attributed to the disentanglement of polymer chains. Consistently, a MD simulation study of the deformation of an amorphous polyethylene revealed [8] that the energy of the non-bonded inter-chain significantly changes the accompanying strain-softening behavior. However, this disentanglement process is not consistent with the viscoelastic behavior in the crept a-Se. The possible reason for the missing of the disentanglement-induced viscoelasticity in a-Se may be the short length of Se chains. Besides the non-bonded interaction change, MD simulation revealed [8] that the energy component associated with the dihedral angular torsion is significantly reduced when polymer is under deformation especially at a relatively high temperature or low strain rate. Since the average intra- and inter-atomic distances do not change at all, it is conceivable that the abnormal anisotropic intensity in the crept a-Se is related to bond rotation, i.e., the change of the dihedral angle. This bond-rotation-induced viscoelasticity can be understood through Fig. 4b. Helixlike segments in Se chains are preferred conformations with low energy [35]. When a-Se is under shear, helixlike segments become to ringlike conformations [35] simply by the change of the dihedral angle, as illustrated in the Fig. 4b. Note that the bond angle remains unchanged. Otherwise, the second intra-chain nearest atomic distance would change. As a consequence of this conformation rearrangement, more bonds are perpendicular to the loading axis, different from the Zr-MG case involving the topological rearrangement. The conformation change in amorphous Se arises from the rotational degree of freedom around the single chemical bonds connecting the backbone atoms while the topological rearrangements involve bond break and formation. Therefore, the anisotropic distribution of the Se-Se bonds in space caused the unique intensity anisotropic diffraction pattern, as shown in Fig. 1b. The MD simulation has shown that ringlike segments are rare in the a-Se because of the steric hindrance effect [35]. Distinct from the confined flow defects in Zr-MG, structure change induced by viscoelasticity does not produce back stress. The structure change, instead, in a-Se is purely conformation change. Conformational entropy is the entropy associated with the number of conformations of a-Se chain structure. After the creep, the number of conformations is reduced

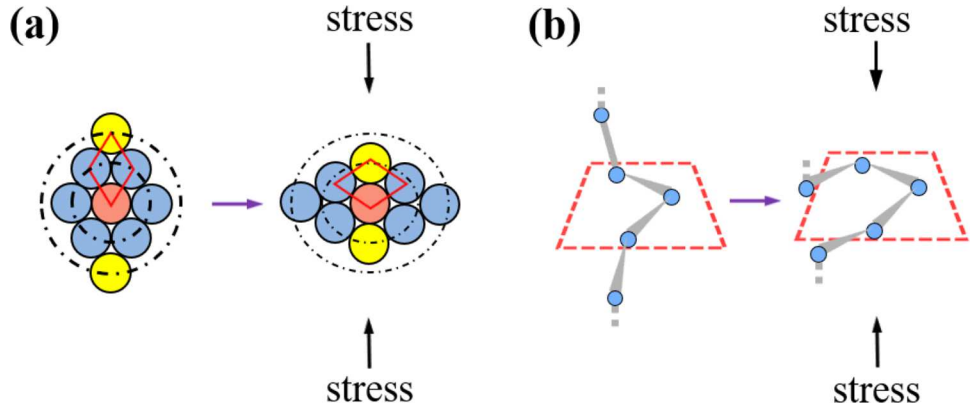

Fig. 4. An illustration of structural change associated with viscoelasticity in the MGs (a) and a-Se (b) under thermal creep. The dash-dot circle indicates the first and second atomic shells. The red rhombus highlights the elementary bond-switch unit in the viscoelastic deformation of MGs.

because the external load drives the a-Se to form ringlike conformation, as illustrated in Fig. 4b. Therefore, the recovery of viscoelasticity in the crept a-Se is entirely driven by entropy increase, distinct from the back stress-driven recovery in MGs.

The free-volume model originally developed for polymers is extended to MGs without considering the structural identity of free-volume defects in MGs. Similar to the polymer case, the individual chains in a-Se sufficiently separate to leave an abundant free volume of monomeric size in between chains, but the free volume in MGs is much smaller than an atomic size because of their densely packed structures. Here, thermal creep introduces structural rejuvenation into the Zr-MG by widening the distribution of atomic distances, rather than simply increasing the atomic distance expected from the free-volume model. It was shown that the height and width of the peaks of $g_0^0(r)$ are associated with the atomic pressure fluctuation, $<P^2>$, (equivalent to the density fluctuation [36]) in MGs [37]. From the perspective of energy, atomic sites under compression (an anti-free volume) or expansion (a free volume) are both unstable, acting as potential structural defects. Apparently, the increase of the density fluctuation observed in the crept Zr-MG results from the creation of both the anti-free volume and free volume. The opposite is true when MGs are annealed [38–40]. Annealing essentially causes a combination of the anti-free volume and free volume, which cancels out the net volume change of MGs. In fact, the MGs' volume change induced by annealing is negligible, less than 0.2% [10–12], which may be related to the anharmonicity of the potential. But MGs' ductility can degrade dramatically after annealing, exhibiting a ductile-to-brittle transition [40].

In summary, viscoelasticity in both Zr-MG and a-Se is associated with the bond-orientation anisotropy, but its corresponding structural change and consequence are dramatically different because of these two materials' unique structural units. Also, our study clearly pointed out that the definition of free-volume defects varies from MGs to amorphous nonmetallic materials, at least a-Se, and is closely related to the packing density of individual structural units. The difference of the structural change in these two materials causes the divergence of the recovery effect of viscoelasticity: the memory effect in a-Se is driven by the entropy whereas the viscoelasticity in MGs is recovered by the elastic field.

Declaration of Competing Interest

The authors declare that they have no known competing financial interests or personal relationships that could have appeared to influence the work reported in this paper.

Acknowledgement

Y.Tong gratefully acknowledge the financial support by the National Natural Science Foundation of China (NSFC) (Grant No. 52001272). P. K. Liaw very much appreciates the support from the National Science Foundation (DMR-1611180 and 1809640) with program directors, Drs. J. Yang, G. Shiflet, and D. Farkas. This research used resources of the Advanced Photon Source, a U.S. Department of Energy (DOE) Office of Science user facility operated for the DOE Office of Science by Argonne National Laboratory under Contract No. DE-AC02-06CH11357.

References

[1] W.H. Wang, Y. Yang, T.G. Nieh, C.T. Liu, Intermetallics 67 (2015) 81.
[2] Z. Wang, B.A. Sun, H.Y. Bai, W.H. Wang, Nat. Commun. 5 (2014) 5823.
[3] J.S. Harmon, M.D. Demetriou, W.L. Johnson, K. Samwer, Phys. Rev. Lett. 99 (2007) 4.
[4] Y. Tong, T. Iwashita, W. Dmowski, H. Bei, Y. Yokoyama, T. Egami, Acta Mater. 86 (2015) 240.
[5] Y. Tong, PhD Diss, Uiversity of Tennessee, 2015.
[6] A.S. Argon, Acta Metall. 27 (1979) 11.
[7] A.S. Argon, Acta Metall. 31 (1983) 499.
[8] D. Hossain, M.A. Tschopp, D.K. Ward, J.L. Bouvard, P. Wang, M.F. Horstemeyer, Polymer 51 (2010) 6071.
[9] J.S. Langer, Phys. Rev. E 77 (2008), 021502.
[10] Y. Yokoyama, T. Yamasaki, P.K. Liaw, A. Inoue, Acta Mater. 56 (2008) 6097.
[11] O. Haruyama, K. Kisara, A. Yamashita, K. Kogure, Y. Yokoyama, K. Sugiyama, Acta Mater. 61 (2013) 3224.
[12] M. Kohda, O. Haruyama, T. Ohkubo, T. Egami, Phys. Rev. B 81 (2010), 092203.
[13] P.Y. Huang, S. Kurasch, A. Srivastava, V. Skakalova, J. Kotakoski, A. V. Krasheninnikov, R. Hovden, Q. Mao, J.C. Meyer, J. Smet, D.A. Muller, U. Kaiser, Nano Lett. 12 (2012) 1081.
[14] T.C. Hufnagel, R.T. Ott, J. Almer, Phys. Rev. B 73 (2006) 8.
[15] D.B. Miracle, Nat. Mater. 3 (2004) 697.
[16] E.M. Y.Q.Cheng, Prog. Mater. Sci. 56 (2011) 95.
[17] M.H. Cohen, D. Turnbull, J. Chem. Phys. 31 (1959) 1164.
[18] T. Iwashita, T. Egami, Phys. Rev. Lett. 108 (2012).
[19] A.P. Hammersley, S.O. Svensson, A. Thompson, Nucl. Instrum. Methods A 346 (1994) 10.
[20] W. Dmowski, T. Egami, Adv. Eng. Mater. 10 (2008) 5.
[21] F.O. Mear, G. Vaughan, A.R. Yavari, A.L. Greer, Phil. Mag. Lett. 88 (2008) 757.
[22] H.F. Poulsen, J.A. Wert, J. Neuefeind, V. Honkimaki, M. Daymond, Nat. Mater. 4 (2005) 33.
[23] Y. Tong, K. Jin, H. Bei, J.Y.P. Ko, D.C. Pagan, Y. Zhang, F.X. Zhang, Mater. Des. 155 (2018) 1.
[24] J. Bohlen, M.R. Nürnberg, J.W. Senn, D. Letzig, S.R. Agnew, Acta Mater. 55 (2007) 2101.
[25] J.J. Lewandowski, A.L. Greer, Nat. Mater. 5 (2006) 15.
[26] Y. Suzuki, T. Egami, J. Non-Cryst. Solids 75 (1985) 6.
[27] W. Dmowski, T. Egami, J. Mater. Res. 22 (2007) 7.
[28] W. Dmowski, T. Iwashita, C.-.P. Chuang, J. Almer, T. Egami, Phys. Rev. Lett. 105 (2010), 205502.
[29] W. Dmowski, Y. Yokoyama, A. Chuang, Y. Ren, M. Umemoto, K. Tsuchiya, A. Inoue, T. Egami, Acta Mater. 58 (2010) 10.
[30] T. Egami, Prog. Mater. Sci. (56) (2011) 637.
[31] H. Poulsen, J. Wert, J. Neuefeind, V. Honkimaki, M. Daymond, Nat. Mater. 4 (2005) 4.
[32] J. Hegedus, S. Kugler, J. Optoelectron. Adv. M. 7 (2005) 1923.
[33] Y. Suzuki, J. Haimovich, T. Egami, Phys. Rev. B 35 (1987) 7.
[34] W. Dmowski, Y. Tong, T. Iwashita, Y. Yokoyama, T. Egami, Phys. Rev. B 91 (2015), 060101.
[35] K. Nakamura, A. Ikawa, Phys. Rev. B 67 (2003), 104203.
[36] T. Egami, D. Srolovitz, J. Phys. F 12 (1982) 2141.
[37] D. Srolovitz, T. Egami, V. Vitek, Phys. Rev. B 24 (1981) 9.
[38] T. Egami, J. Mater. Sci. 13 (1978) 2587.
[39] W. Dmowski, C. Fan, M.L. Morrison, P.K. Liaw, T. Egami, Mater. Sci. Eng. A 471 (2007) 125.
[40] Y. Tong, W. Dmowski, Y. Yokoyama, G. Wang, P.K. Liaw, T. Egami, Scripta Mater. 69 (2013) 570.